JOURNAL OF

Photochemistry and Photobiology

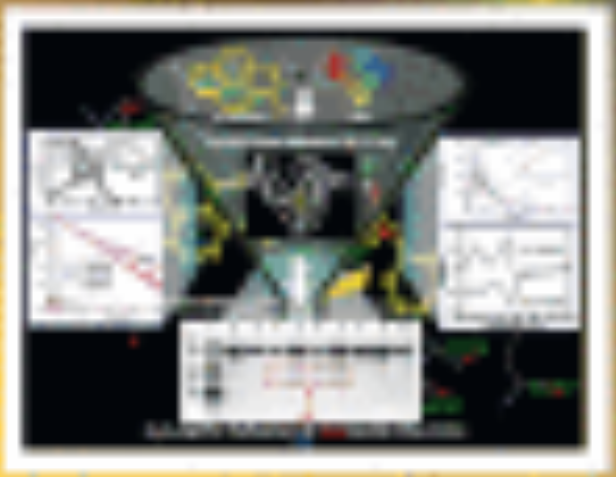

A: Chemistry

Journal of
Photochemistry and Photobiology
A:Chemistry

Volume 340 (2017)

Asian Editor
O. Ishitani
(Tokyo, Japan)

Associate Editor to Asian Editor
R. Abe
(Kyoto, Japan)

European Editor
S. Meech
(Norwich, UK)

American Editor
J. Sivaguru
(Fargo, ND, USA)

Assistant Editors
G. Yang
(Beijing, China)
Y. Li
(Beijing, China)

Founding Editor
R.P. Wayne
(Oxford, UK)

Editorial Board
N.S. Allen (*Manchester, UK*)
D. (D) Bahnemann *(Hannover, Germany)*
S. Campagna (*Messina, Italy)*
S.M.B. Costa (*Lisbon, Portugal*)
A. Douhal (*Toledo, Spain*)
M. Forbes (*Bowling, Ohio, USA*)
H. Fukumura (*Sendai, Japan*)
K. Ghiggino (*Melbourne, Australia*)
D. Guldi (*Erlangen, Germany*)
B. Heyne (*Calgary, Canada*)
J. Hofkens (*Leuven, Belgium*)
H. Inoue (*Tokyo, Japan*)
M. Irie (*Tokyo, Japan*)
J. Karpiuk (*Warszawa, Poland*)
A.G. Kutateladze (*Denver, Colorado, USA*)
H. Masuhara (*Hsinchu, Taiwan*)
A. Mills (*Glasgow, UK*)
J.P. Mittal (*Mumbai, India*)
H. Miyasaka (*Osaka, Japan*)
K. Mizuno (*Osaka, Japan*)
K. Nakatani *(Cachan, France)*
E.T.J. Nibbering (*Berlin, Germany*)
B. Ohtani (*Sapporo, Japan*)
J.C. Polanyi (*Toronto, Ont., Canada*)
J. Rack (*Albuquerque, New Mexico, USA*)
V. Ramamurthy (*Coral Gobles, FL, USA*)
F. Raymo (*Coral Gables, Florida, USA*)
J.C. Scaiano (*Ottawa, Ont., Canada*)
G. Scholes (*Princeton, New Jersey, USA*)
Linda (L.) Shimizu (*South Carolina, USA*)
R.P. Steer (*Saskatoon, Sask., Canada*)
V. Sundström (*Lund, Sweden*)
C.H. Tung (*Beijing, China*)
M. Wasielewski (*Evanston, IL, USA*)
V.W.W. Yam (*Hong Kong, PR China*)

Processed at Thomson Digital, Gangtok (India)

ELSEVIER

Amsterdam • Boston • London • New York • Oxford •
Paris • Philadelphia • San Diego • St. Louis

JOURNAL OF PHOTOCHEMISTRY AND PHOTOBIOLOGY A: CHEMISTRY

Asian Editor
O. Ishitani (*Tokyo, Japan*)

Associate Editor to Asian Editor
R. Abe (*Kyoto, Japan*)

European Editor
S. Meech (*Norwich, UK*)

American Editor
J. Sivaguru (*Fargo, ND, USA*)

Assistant Editors
G. Yang *(Beijing, China)*
Y. Li *(Beijing, China)*

Editorial Board
N.S. Allen (*Manchester, UK*)
D. (D) Bahnemann *(Hannover, Germany)*
S.M.B. Costa (*Lisbon, Portugal*)
A. Douhal (*Toledo, Spain*)
M. Forbes (*Bowling, Ohio, USA*)
H. Fukumura (*Sendai, Japan*)
K. Ghiggino (*Melbourne, Australia*)
D. Guldi (*Erlangen, Germany*)
B. Heyne (*Calgary, Canada*)
J. Hofkens (*Leuven, Belgium*)
H. Inoue (*Tokyo, Japan*)
M. Irie (*Tokyo, Japan*)
J. Karpiuk (*Warszawa, Poland*)
A.G. Kutateladze (*Denver, Colorado, USA*)
H. Masuhara (*Hsinchu, Taiwan*)
A. Mills (*Glasgow, UK*)
J.P. Mittal (*Mumbai, India*)
H. Miyasaka (*Osaka, Japan*)
K. Mizuno (*Osaka, Japan*)
K. Nakatani *(Cachan, France)*
E.T.J. Nibbering (*Berlin, Germany*)
B. Ohtani (*Sapporo, Japan*)
J.C. Polanyi (*Toronto, Ont., Canada*)
J. Rack (*Albuquerque, New Mexico, USA*)
V. Ramamurthy (*Coral Gobles, FL, USA*)
F. Raymo (*Coral Gables, Florida, USA*)
J.C. Scaiano (*Ottawa, Ont., Canada*)
G. Scholes (*Princeton, New Jersey, USA*)
Linda (L.) Shimizu (*South Carolina, USA*)
R.P. Steer (*Saskatoon, Sask., Canada*)
V. Sundström (*Lund, Sweden*)
C.H. Tung (*Beijing, China*)
M. Wasielewski (*Evanston, IL, USA*)
V.W.W. Yam (*Hong Kong, PR China*)

Founding Editor
R.P. Wayne (*Oxford, UK*)

Aims & Scope

JPPA publishes the results of fundamental studies on all aspects of chemical phenomena induced by interactions between light and molecules/matter of all kinds.

All systems capable of being described at the molecular or integrated multimolecular level are appropriate for the journal. This includes all molecular chemical species as well as biomolecular, supramolecular, polymer and other macromolecular systems, as well as solid state photochemistry. In addition, the journal publishes studies of semiconductor and other photoactive organic and inorganic materials, photocatalysis (organic, inorganic, supramolecular and superconductor).

The scope includes condensed and gas phase photochemistry, as well as synchrotron radiation chemistry. A broad range of processes and techniques in photochemistry are covered such as light induced energy, electron and proton transfer; nonlinear photochemical behavior; mechanistic investigation of photochemical reactions and identification of the products of photochemical reactions; quantum yield determinations and measurements of rate constants for primary and secondary photochemical processes; steady-state and time-resolved emission, ultrafast spectroscopic methods, single molecule spectroscopy, time resolved X-ray diffraction, luminescence microscopy, and scattering spectroscopy applied to photochemistry. Papers in emerging and applied areas such as luminescent sensors, electroluminescence, solar energy conversion, atmospheric photochemistry, environmental remediation, and related photocatalytic chemistry are also welcome.

JPPA publishes Regular Articles, Invited Feature Articles, and Short Notes. Regular Articles allow for a complete overview of research results. Specialist researchers will be occasionally invited by Editors to write Invited Feature Articles. Alternatively, proposals for Invited Feature Articles may be submitted by e-mail to one of the Editors for consideration. Invited Feature Articles are intended to present an overview of the author's recent work in relation to other published research in the field, and are not intended to be a comprehensive overview of a particular sub-discipline. Short Notes are 2-page papers with relevant new results, data or technical reports that are important to the photochemistry community.

Papers that are only minor extensions of previous work or contain mainly descriptions of the synthesis of molecules or materials without a detailed photochemistry study will not be accepted for publication.

Prospective authors of review articles are kindly advised to consult the Journal of Photochemistry and Photobiology C: Photochemistry Reviews and follow manuscript preparation instructions as described at http://www.elsevier.com/locate/jphotochemrev.

Processed at Thomson Digital, Gangtok (India)

Frequency
Eighteen volumes in 2017.

Publication information: *Journal of Photochemistry and Photobiology A: Chemistry* (ISSN 1010-6030) publishes eighteen volumes per year by Elsevier (Radarweg 29, 1043 NX Amsterdam, the Netherlands). Further information on this journal is available from the Publisher or from the Elsevier Customer Service Department nearest you or from this journal's website (http://www.elsevier.com/locate/jphotochem). Information on other Elsevier products is available through Elsevier's website (http://www.elsevier.com). Periodicals Postage Paid at Rahway, NJ, and at additional mailing offices.

Orders, claims, and journal enquiries:
Please contact the Elsevier Customer Service Department nearest you:

St. Louis:
Elsevier Customer Service Department, 3251 Riverport Lane, Maryland Heights, MO 63043, USA; phone: (877) 8397126 [toll free within the USA]; (+1) (314) 4478878 [outside the USA]; fax: (+1) (314) 4478077; e-mail: JournalCustomerService-usa@elsevier.com

Oxford:
Elsevier Customer Service Department, The Boulevard, Langford Lane, Kidlington, Oxford OX5 1GB, UK; phone: (+44) (1865) 843434; fax: (+44) (1865) 843970; e-mail: JournalsCustomerServiceEMEA@elsevier.com

Tokyo
Elsevier Customer Service Department, 4F Higashi-Azabu, 1-Chome Bldg,1-9-15 Higashi-Azabu, Minato-ku,Tokyo106-0044, Japan, phone: (+81) (3) 55615037; fax: (+81) (3) 55615047; e-mail: JournalsCustomerServiceJapan@elsevier.com

Singapore
Elsevier Customer Service Department, 3 Killiney Road, #08-01 Winsland House I, Singapore 239519, phone: (+65) 63490222; fax: (+65) 67331510; e-mail: JournalsCustomerServiceAPAC@elsevier.com

ADVERTISEMENT

Chemistry jobs
The best jobs in science, technology & medicine
Get hired
Mendeley Careers

ScienceDirect switches to a secure connection January 23rd. Start using HTTPS today.

Search all fields | Author name | --This Journal/Book-- | Volume | Issue | Page | Advanced search

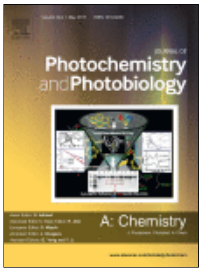

Journal of Photochemistry and Photobiology A: Chemistry

Supports Open Access | About this Journal | Sample Issue Online | Submit your Article

Formerly part of Journal of Photochemistry;

Get new article feed

Get new Open Access article feed

Subscribe to new volume alerts

Add to Favorites

Copyright © 2018 Elsevier B.V. All rights reserved

< Previous vol/iss | Next vol/iss >

Articles in Press

Open Access articles

Volumes 351 - 356 (2018)

Volumes 341 - 350 (2017 - 2018)

Volumes 331 - 340 (2016 - 2017)

Volume 340
pp. 1-202 (1 May 2017)

Volume 339
pp. 1-114 (15 April 2017)

Volume 338
pp. 1-214 (1 April 2017)

Volume 337
pp. 1-216 (15 March 2017)

Volume 336
pp. 1-208 (1 March 2017)

Volume 335
pp. 1-310 (15 February 2017)

Volume 334
pp. 1-112 (1 February 2017)

Volume 333
pp. 1-234 (15 January 2017)

Volume 332
pp. 1-610 (1 January 2017)

Volume 331
pp. 1-254 (1 December 2016)
Special issue in honor of Prof. Yoshihisa Inoue for his contribution on molecular and supramolecular photochemistry

Volumes 321 - 330 (2016)

Volumes 311 - 320 (2015 - 2016)

Volumes 301 - 310 (2015)

Volumes 291 - 300 (2014 - 2015)

Journal of Photochemistry and Photobiology A: Chemistry
Volume 340, Pages 1-202 (1 May 2017)

Purchase | Export | All access types

Pages 96-108
S. Shanavas, A. Priyadharsan, V. Vasanthakumar, A. Arunkumar, P.M. Anbarasan, S. Bharathkumar
Abstract | Graphical abstract | Research highlights | Purchase PDF - $39.95

Characterization, photoelectrochemical properties, and surface wettabilities of transparent porous TiO_2 thin films Original Research Article
Pages 109-119
Li-Heng Kao, Ya-Ping Chen
Abstract | Graphical abstract | Research highlights | Purchase PDF - $39.95

MoS_2-graphene hybrids as efficient counter electrodes in CdS quantum-dot sensitized solar cells Original Research Article
Pages 120-127
Miaomiao Zhen, Fengyan Li, Ran Liu, Chunli Song, Lin Xu, X.Z. Luo
Abstract | Graphical abstract | Research highlights | Purchase PDF - $39.95

Photocatalytic synthesis of reduced graphene oxide-zinc oxide: Effects of light intensity and exposure time Original Research Article
Pages 128-135
Faisal Hussin, Hendrik O. Lintang, Siew Ling Lee, Leny Yuliati
Abstract | Graphical abstract | Research highlights | Purchase PDF - $39.95 | Supplementary content

Facial synthesis of sheet-like carbon nitride from preorganized hydrogen bonded supramolecular precursors and its high efficient photocatalytic oxidation of gas-phase NO Original Research Article
Pages 136-145
Shipeng Wan, Qin Zhong, Man Ou, Shule Zhang, Wei Cai
Abstract | Graphical abstract | Research highlights | Purchase PDF - $39.95 | Supplementary content

Visible active N, S co-doped TiO_2/graphene photocatalysts for the degradation of hazardous dyes Original Research Article
Pages 146-156
Appavu Brindha, Thiripuranthagan Sivakumar
Abstract | Graphical abstract | Research highlights | Purchase PDF - $39.95 | Supplementary content

Microwave assisted synthesis of graphene-$Bi_8La_{10}O_{27}$-Zeolite nanocomposite with efficient photocatalytic activity towards organic dye degradation Original Research Article
Pages 157-169
Yonrapach Areerob, Kwang-Youn Cho, Won-Chun Oh
Abstract | Graphical abstract | Research highlights | Purchase PDF - $39.95

Wirelike dinuclear ruthenium(II)polyterpyridine complexes based on D–P–A architecture: Experimental and theoretical investigation Original Research Article
Pages 170-180
Pallavi Singh, Prem Jyoti Singh Rana, Prasenjit Kar
Abstract | Graphical abstract | Research highlights | Purchase PDF - $39.95 | Supplementary content

< Previous vol/iss | Next vol/iss >

About ScienceDirect Remote access Shopping cart Contact and support Terms and conditions Privacy policy

Cookies are used by this site. For more information, visit the cookies page.
Copyright © 2018 Elsevier B.V. or its licensors or contributors. ScienceDirect ® is a registered trademark of Elsevier B.V.

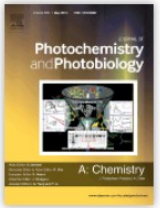

ISSN: 1010-6030

Journal of Photochemistry and Photobiology A: Chemistry

› Supports Open Access

Regional Editors: S. Meech, J. Sivaguru, O. Ishitani:

› View Editorial Board

JPPA publishes the results of fundamental studies on all aspects of chemical phenomena induced by interactions between light and molecules/matter of all kinds.

All systems capable of being described at the molecular or integrated multimolecular level are appropriate for the journal. This includes all...

Read more

Submit Your Paper

View Articles

Guide for Authors

Abstracting/ Indexing

Track Your Paper

Order Journal

Sample Issue

Most Downloaded | Recent Articles | Most Cited | Open Access Articles

An overview of semiconductor photocatalysis Andrew Mills | Stephen Le Hunte

What is Degussa (Evonik) P25? Crystalline composition analysis, reconstruction from isolated pure particles and photocatalytic activity test B. Ohtani | O.O. Prieto-Mahaney | ...

Concurrent synthesis of nitrogen-doped carbon dots for cell imaging and ZnO@nitrogen-doped carbon sheets for photocatalytic degradation of methylene blue Raji Atchudan | Thomas Nesakumar Jebakumar Immanuel Edison | ...

› View All Most Downloaded Articles

Journal Metrics

CiteScore: **2.60**

More about CiteScore

Impact Factor: **2.625**

5-Year Impact Factor: **2.493**

Source Normalized Impact per Paper (SNIP): **0.841**

SCImago Journal Rank (SJR): **0.732**

› View More on Journal Insights

Your Research Data

› Share your research data

› Visualize your data

Mendeley Data

The latest Mendeley datasets for Journal of Photochemistry and Photobiology A: Chemistry.

Data for: Microwave assisted synthesis of Ta_2O_5 nanostructures for photocatalytic hydrogen production

Michael Wark | Dereje H. Taffa | ...

1 file (2018)

Data for: Wavelength Dependent Photochemistry of Expanded Chromophore and Asymmetric Dibenzothiophene S-Oxides Derivatives

Ryan McCulla | John Petroff

Journal of Photochemistry and Photobiology A: Chemistry 340 (2017) 128–135

Contents lists available at ScienceDirect

Journal of Photochemistry and Photobiology A: Chemistry

journal homepage: www.elsevier.com/locate/jphotochem

Photocatalytic synthesis of reduced graphene oxide-zinc oxide: Effects of light intensity and exposure time

Faisal Hussin[a], Hendrik O. Lintang[b,c], Siew Ling Lee[a,b], Leny Yuliati[b,c,*]

[a] Department of Chemistry, Faculty of Science, Universiti Teknologi Malaysia, 81310, UTM, Johor Bahru, Johor, Malaysia
[b] Centre for Sustainable Nanomaterials, Ibnu Sina Institute for Scientific and Industrial Research, Universiti Teknologi Malaysia, 81310, UTM, Johor Bahru, Johor, Malaysia
[c] Ma Chung Research Center for Photosynthetic Pigments, Universitas Ma Chung, Villa Puncak Tidar N-01, Malang 65151, East Java, Indonesia

ARTICLE INFO

Article history:
Received 5 January 2017
Received in revised form 18 February 2017
Accepted 12 March 2017
Available online 18 March 2017

Keywords:
rGO-ZnO
Photocatalytic reduction
Light intensity
Exposure time
Defect
Charge transfer

ABSTRACT

A series of composites containing reduced graphene oxide and zinc oxide (rGO-ZnO) with optimum GO loading amount of 3 wt% was successfully synthesized through an *in-situ* photocatalytic reduction of graphene oxide (GO) over ZnO photocatalyst under UV light irradiation. Different light intensities and exposure times were confirmed to affect the properties and photocatalytic performance of the rGO-ZnO for photocatalytic degradation of phenol as an organic pollutant model. The best photocatalyst was obtained under UV light intensity of 0.4 mW cm^{-2} for 24 h exposure and it gave around three times higher photocatalytic performance than that of the bare ZnO. Compensating for the long exposure time, such low light intensity was crucial to generate rGO with low amount of defects. The low amount of defects resulted in low electron-hole recombination, low resistance of a charge transfer, and high electron-transfer rate constant, which in turn enhanced the photocatalytic performance. Reusability tests demonstrated the potential use of rGO-ZnO as a good photocatalyst for organic pollutant degradations.
© 2017 Elsevier B.V. All rights reserved.

1. Introduction

Owing to the issues on the water treatment and energy sustainability, exploration on the highly efficient photocatalysts for treating wastewater containing harmful organic pollutants is immensely reported worldwide. In recent decades, zinc oxide (ZnO) has been an attractive photocatalyst [1–10] due to its excellent and remarkable physicochemical properties, including wide band gap (3.37 eV), chemical inertness, and strong oxidation ability. While the photocorrosion under solar light can be neglected [1], ZnO suffered to photocorrosion when illuminated under UV light irradiation [2–7,11], and it has a high rate of charge recombination, which practically hindered its applications for numerous types of reactions. In order to suppress the drawbacks of ZnO, many attempts were made to increase the performance of ZnO by modifications with dopants, carbon materials, semiconductor coupling, and dye sensitization [2,11–17].

One of the recent promising modifiers is graphene-based materials. This two-dimensional (2D) material has been put to use especially as the modifier for photocatalysts, owing to its exceptionally unique characters, such as high electron conductivity, excellent mechanical properties, large specific surface area and high thermal stability [18–23]. Despite of the exceptional properties of graphene (GR), graphene oxide (GO) is more favourable as the modifier since oxygen functional groups are important to produce stronger interaction in the hybrid composite photocatalysts [24,25]. However, as GO itself is an insulator, in order to restore the electron conductivity of GO sheets, it is usually partially reduced to reduced graphene oxide (rGO).

The rGO-ZnO composite has been commonly synthesized by several strategies, such as microwave-assisted reaction, hydrothermal, solvothermal, hydrolysis methods, thermal expansion of GO under inert atmosphere by nitrogen, surface coating and liquid arc discharge [26–32]. Unfortunately, the implementation of heat treatment is less favourable since it forms rGO with less crystalline structure and more defects. Thermal expansion of GO under nitrogen and hydrogen atmospheres at lower temperature might overcome the less crystalline of formed rGO. However, it causes a complete reduction of oxygen functionalities on the GO structure, which is less desired since oxygen functionalities are crucial to

* Corresponding author at: Ma Chung Research Center for Photosynthetic Pigments, Universitas Ma Chung, Villa Puncak Tidar N-01, Malang 65151, East Java, Indonesia.
E-mail address: leny.yuliati@machung.ac.id (L. Yuliati).

http://dx.doi.org/10.1016/j.jphotochem.2017.03.016
1010-6030/© 2017 Elsevier B.V. All rights reserved.

provide interactions with ZnO. Moreover, the reduction of GO to rGO by using toxic reducing agents such as hydrazine (N_2H_4) introduced residue of reductant into the rGO suspension. On the other hand, liquid arc discharge method can successfully create high quality of rGO, but further purification is needed to remove the unwanted carbon. Therefore, an alternative strategy using UV light to assist the reduction process in the presence of suitable photocatalyst should be adopted.

Williams *et al.* first demonstrated a clean and environmental-friendly reduction method to convert GO to rGO using ZnO as photocatalyst under UV light irradiation at room temperature [33]. This approach has some valuable advantages. For examples, this method did not use toxic reducing agents, did not produce any impurities and produce partially reduced oxygen functionalities on rGO structure which are useful on providing interactions between rGO and ZnO. This method also offered mild conditions for the synthesis process. The photocatalytic property of the rGO-ZnO prepared by this mild method was first reported for reduction of Cr (VI) [34]. It was obtained that the rGO-ZnO composite gave 1.5 times higher photocatalytic activity than that of the bare ZnO since the electron-hole recombination on ZnO was successfully suppressed and the light absorption capability was improved in the presence of the rGO.

Herein, we reported the effects of light intensity and exposure time on the properties and performance of rGO–ZnO composites prepared by the reduction method carried out photocatalytically over the ZnO as the photocatalyst. Light intensity and exposure time are considered to be crucial to prepare the rGO-ZnO composites, which however, have never been addressed yet. The use of strong light intensity might lead to the extensive reduction or destruction of GO. On the other hand, the duration of the synthesis time shall be also optimized for efficiency and avoiding the over-reduction of the GO. Notably, we could obtain the rGO-ZnO with much better photocatalytic performance (3.4 times) as compared to the bare ZnO when it was synthesized using low UV light intensity (0.4 mW cm^{-2}) and enough irradiation time (24 h). The superior photocatalytic performance of the composite was strongly related to formation of defects in low amount that promoted charge separation and improved electron charge transfer between the rGO and the ZnO, as evidenced by Raman, electrochemical impedance spectroscopies (EIS), and photocurrent investigations.

2. Experimental

2.1. Synthesis of ZnO

ZnO was synthesized by a simple co-precipitation method according to the reported literature [3] using zinc acetate dehydrate ($Zn(CH_3COO)_2{\cdot}2H_2O$, 99.5%, QRëc) as the starting precursor. Briefly, the $Zn(CH_3COO)_2{\cdot}2H_2O$ (4.5 g) was dissolved in deionized water (100 mL) and then sonicated for 30 min to obtain solution A. In order to prepare solution B, sodium hydroxide (NaOH, 99%, QRëc, 6.4 g) was dissolved in deionized water (100 mL) and hexadecyltrimethylammonium bromide ($(C_{16}H_{33})N(CH_3)_3Br$, 99%, Merck, 7.28 g) was added into the solution, followed by stirring for 1 h to make the solution homogeneous. Subsequently, the solution A was added slowly into the solution B and then heated at 70 °C for 1 h. The remaining solid was filtered and washed by deionized water and ethanol, consecutively. The as-prepared ZnO was dried and calcined at 500 °C in air with a ramp rate of 1.0 °C min^{-1} and further tempered for another 1 h at this temperature. The resulting white solid was subsequently ground to get the ZnO powder.

2.2. Synthesis of GO

The improved Hummers' method was adopted to synthesize GO [35]. Graphite flakes (C, 99%, Merck, 1 g) and potassium permanganate ($KMnO_4$, 99.5%, 6 g) were added into a 500 mL of round bottom flask, followed by addition of concentrated sulphuric acid (H_2SO_4, >95%, Fisher Scientific, 135 mL) and phosphoric acid (H_3PO_4, 85%, Merck, 15 mL) with ratio of 9:1. The mixture was stirred at 50 °C for 24 h. Upon completion of reaction and cooling to room temperature, it was poured into ice water (400 mL). The solution was quenched with the addition of hydrogen peroxide (H_2O_2, 30%, Fisher Scientific, 5 mL) in order to reduce permanganate that might be remained. The solid was later collected by centrifuging the mixture for about 10 min (4000 rpm). The solid obtained was further washed two times with hydrochloric acid (HCl, 30%, Fisher Scientific, 200 mL) and distilled water by centrifugation until pH solution was near to 7, consecutively. Upon reaching pH of 7, the solid was dispersed into methanol (CH_3OH, 99.99%, Fisher Scientific, 100 mL), followed by sonication for 1 h. The solution was then evaporated at 40 °C and vacuum dried overnight at room temperature.

2.3. Synthesis of rGO-ZnO

rGO-ZnO composites were prepared through a photocatalytic reduction method using ZnO as the photocatalyst to reduce GO [34] using different weight ratios of GO, light intensities and duration times. The weight ratios of GO were fixed at 0.5, 1, 3, 5, and 10 wt%. As a typical synthesis of 3 wt% rGO-ZnO, the ZnO (1 g) was dispersed in methanol (CH_3OH, 99.99%, Fisher Scientific, 60 mL) and the prepared GO (0.03 g) was added to the mixture, followed by ultrasonication for 30 min. After sonication, the mixture was then exposed under UV light irradiation with a specific condition. The mixture was then filtered and subsequently washed by double distilled water and ethanol. The obtained solid was further dried at 60 °C in an oven overnight. The 3 wt% rGO-ZnO sample was labelled as rGO(a,b)-ZnO, where a showed the light intensity of UV light with a varying from 0.2 to 13.0 mW cm^{-2}, while b represented the time exposure during photocatalytic reduction with b varying from 3 to 24 h.

2.4. Characterizations

The crystal structure of the synthesized rGO-ZnO composites was analysed by an X-ray diffractometer (XRD) using a Bruker Advance D8 diffractometer with Cu K_α radiation (λ = 1.5406 Å) at a scan rate of 0.05 ° s^{-1}. The applied current and accelerating voltage used were 40 mA and 40 kV, respectively. The Fourier transform infrared (FTIR) spectra of the prepared composites were recorded by a Thermo Scientific Nicolet iS50 using pellet technique with potassium bromide (KBr). The stability of prepared sample and weight content analysis of rGO was analysed with a thermogravimetric analyzer (TGA) using a Mettler TGA/SDTA 851^e. The samples were heated from 50 to 800 °C with a heating rate of 10 °C min^{-1}. In order to study the morphology of the samples, transmission electron microscope (TEM) images were recorded on a JEOL JEM-2100, which an accelerating voltage was set to 200 kV. The diffuse reflectance ultraviolet-visible (DR UV–vis) spectra were investigated by a Shimadzu UV-2600. Barium sulphate ($BaSO_4$) was used as the reflectance standard. The fluorescence spectra of samples were measured at room temperature on a fluorescence spectrophotometer (JASCO, FP-8500). Both of excitation and emission bandwidths were fixed at 5 nm. Raman spectra of the prepared samples were measured by an XploRA Plus Raman Microscope HORIBA with the selected laser wavelength of 532 nm.

2.5. Photocatalytic performances

Photocatalytic performances of the rGO-ZnO composites were investigated for the degradation of phenol (C_6H_5OH, 99.5%, Scharlau) under 6 h of UV light irradiation. Self-degradation of phenol was also tested under UV light but without the presence of photocatalyst. Initially, the photocatalyst sample (0.05 g) was dispersed into a solution of phenol (50 mL, 10 ppm in acetonitrile (C_2H_3N, 99.9%, Merck). The 8 W UV lamp ($I = 0.4\ mW\ cm^{-2}$) was used for all the photocatalytic activity tests. Before light exposure, the dark condition was performed by stirring the suspension for 30 min to achieve adsorption-desorption equilibrium between the sample and phenol. An open system was implemented at all the photocatalytic reactions. After reaction, remained phenol was analysed by a Gas Chromatography (GC, Agilent Technologies 7820A) system using a flame ionization detector (FID). The degradation of phenol was evaluated based on the percentage ratio of degraded concentration after and prior the reaction. As for the photostability tests, the rGO(0.4,24)-ZnO composite was reused as the photocatalyst for three successive cycles.

2.6. Electrochemical and photoelectrochemical measurements

2.6.1. Electrode preparation

The screen-printed electrode (SPE, DS 110) was used for both electrochemical and photoelectrochemical measurements. Silver was invoked as the reference electrode, while carbon was used as both the working and counter electrode. As for the electrode preparation, deionized water (1 mL) was mixed with Nafion®117 solution (10 μL, 99%, Sigma Aldrich) and the as-obtained sample (0.01 g) was introduced into the solution. In order to produce a good dispersion, the mixture was ultrasonicated for about 10 min. A small amount of the supernatant (20 μL) was dropped onto the SPE. The SPE was then manually dried with a dryer before using it.

2.6.2. EIS measurement

EIS data were measured on a Gamry Interphase 1000. As the electrolyte, a mixture of potassium ferricyanide ($K_3[Fe(CN)_6]$, 98.5%, Sigma Aldrich, 2.5 mM) and sodium sulphate (Na_2SO_4, 98.5%, QRëc, 0.1 M) was prepared as aqueous solution (6 mL). For measurements of Nyquist plots, the amplitude was fixed at 10 mV, while the frequency range of 0.1–1 MHz. All the measurements were conducted using the same amount of sample loading and under the similar conditions.

2.6.3. Transient photocurrent measurement

The photocurrent data were collected using a chronoamperometry. All measurements were performed under UV light irradiation (8 W, $I = 0.4\ mW\ cm^{-2}$) using the same amount of sample, electrode and electrolyte amounts. For photocurrent plot, the interval for each on-off process used was 30 s.

3. Results and discussion

3.1. Photocatalytic performances

Preliminary studies were conducted in order to obtain the optimum loading of GO for phenol degradation. Dark condition was carried out to ensure equilibrium of adsorption-desorption was reached. It was confirmed that no significant adsorption of phenol could be detected for all samples, suggesting that the introduction of GO did not improve adsorption capability of the ZnO. As shown in Table S1, the photocatalytic activity observed for bare ZnO after 6 h photocatalytic reaction was 9%. After modification with GO, the activity was significantly increased up to 31% when the GO loading reached its optimum amount at 3 wt%. However, higher GO loading above 3 wt% led to lower photocatalytic activity, which might be due to the masking effect of GO. Even though the decrease in the activity was observed, the performance was still superior as compared to the bare ZnO. This result clearly showed that the addition of GO indeed improved the photocatalytic performance of ZnO. Since no degradation of phenol can be observed without photocatalysts, it signifies that the degradation process of phenol was mainly derived from photocatalytic reaction.

Further investigations on the effects of light intensity and exposure time were carried out on the best photocatalyst, which was the 3 wt% rGO-ZnO. The photocatalytic performance of ZnO and rGO(a,b)-ZnO samples prepared under different light intensities (a) and exposure time (b) was tested for degradation of phenol under UV light irradiation. The photocatalytic activities of the ZnO and the rGO-ZnO samples are shown in Table 1. It was clearly observed that all rGO-ZnO samples exhibited significant enhanced photocatalytic activity when compared to the ZnO that only gave 9% degradation (Table 1, entry 1). When the light intensity of $0.4\ mW\ cm^{-2}$ was employed (entries 2–6), the rGO(0.4,24)-ZnO sample prepared under 24 h irradiation gave the highest activity of 31% (entry 5). This result showed that for such low light intensity, 24 h was the required time to generate the most active photocatalyst. Prolonging the exposure time to 30 h caused the activity slightly dropped to 28% (entry 6). Employing exposure time of 24 h, various low light intensities from 0.2 to $0.5\ mW\ cm^{-2}$ were used to synthesize the rGO-ZnO samples. The photocatalytic activities of these samples are also listed down in Table 1 (entries 7–9). It was obvious that the composites prepared using low light intensities gave similar level of photocatalytic activities, which the rGO (0.4,24)-ZnO gave slightly better activity than the others.

The correlation between the irradiation time and light intensities was observed more clearly when the light intensities of 4 (entries 10–13) and $13\ mW\ cm^{-2}$ (entries 14–17) were applied. The shorter duration time (6 h) was found to be the optimum exposure time when using higher light intensity of 4 or 13 mW cm^{-2}. These results obviously indicated that both light intensity and the light irradiation time were correlated to each other to form active photocatalyst, as illustrated in Fig. 1. In order to clarify the effects of light intensity and the length of the irradiation time during synthesis process, and the role of rGO in obtaining the high activity, the best samples for each series of rGO-ZnO composites were selected for further characterizations.

Table 1
Photocatalytic degradation of phenol over ZnO and rGO(a,b)-ZnO samples under UV light irradiation for 6 h.

Entry	Sample	Phenol degradation (%)
1	ZnO	9
2	rGO (0.4,3)-ZnO	18
3	rGO (0.4,6)-ZnO	21
4	rGO (0.4,12)-ZnO	25
5	rGO (0.4,24)-ZnO	31
6	rGO (0.4,30)-ZnO	28
7	rGO (0.2,24)-ZnO	29
8	rGO (0.3,24)-ZnO	30
9	rGO (0.5,24)-ZnO	30
10	rGO (4,3)-ZnO	15
11	rGO (4,6)-ZnO	22
12	rGO (4,12)-ZnO	20
13	rGO (4,24)-ZnO	18
14	rGO (13,3)-ZnO	15
15	rGO (13,6)-ZnO	20
16	rGO (13,12)-ZnO	18
17	rGO (13,24)-ZnO	14

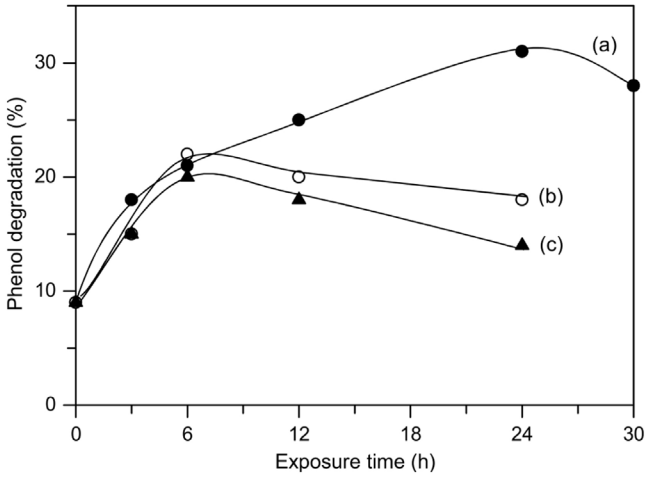

Fig. 1. Effect of light intensity and exposure time during synthesis of rGO-ZnO samples on the photocatalytic degradation of phenol. Light intensities used were (a) 0.4, (b) 4, and (c) 13 mW cm^{-2}.

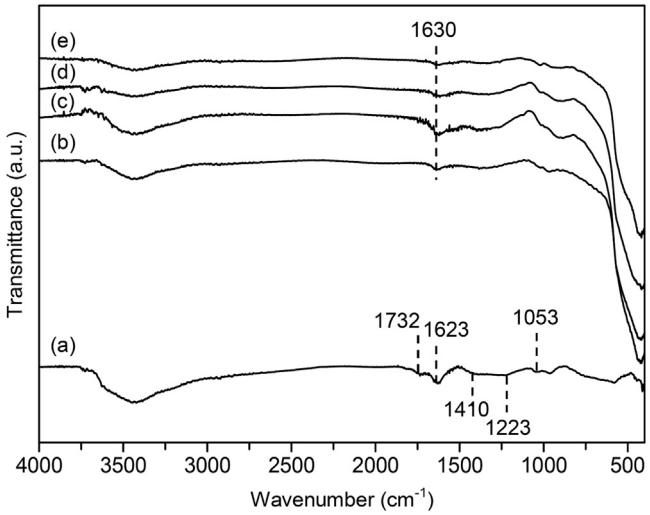

Fig. 3. FTIR spectra of (a) GO, (b) ZnO, (c), rGO(0.4,24)-ZnO, (d) rGO(4,6)-ZnO, and (e) rGO(13,6)-ZnO samples.

3.2. Structure and morphology

The structural properties of GO, ZnO and rGO-ZnO samples were studied by XRD. As displayed in Fig. 2(a), GO gave a diffraction peak at around 9.85° owing to the presence of (001) plane having interplanar distance of 0.90 nm. Shown in Fig. 2(b) is the XRD pattern of ZnO that can be assigned as a wurtzite structure (JCPDS 36-1451). The dominant peak observed for ZnO sample was (101) plane, suggesting that the preferred orientation crystal growth was in *c*-axis [3]. Fig. 2(c)–(e) show the XRD patterns of rGO-ZnO samples. All the samples exhibited the dominant diffraction peaks of ZnO without any significant changes in the intensity, suggesting that the addition of GO did not disturb the crystal structure of ZnO. Absences of the rGO peaks may imply the low amount of added GO.

The functional groups of the prepared samples were further examined by FTIR spectroscopy. As shown in Fig. 3(a), GO showed broad peaks between 3500 and 3000 cm^{-1} that were assigned to the O—H stretching modes. The peaks appeared at 1732, 1632, 1410, 1223 and 1053 cm^{-1} were attributed to the vibration of C=O stretching in carbonyl groups, C=C in the aromatic parts, C—OH stretching, C—O in epoxy groups, and C—O in alkoxy groups [26–29,33–40]. The presence of all these assigned peaks confirmed the successful transformation of graphite to GO. On the other hand, ZnO gave one intense peak in the fingerprint region of 500–400 cm^{-1} (Fig. 3(b)), which was corresponded to a typical peak of Zn—O stretching mode [26,27,34]. Meanwhile, the bending mode of water gave peak around 1630 cm^{-1} [4]. As illustrated in Fig. 3(c)–(e)), all the rGO-ZnO samples exhibited similar peaks to the ZnO. The presence of rGO peaks was hardly observed due to the low loading amount of GO. However, this result showed that the addition of GO did not disturb the structure of ZnO, as also supported by the XRD patterns aforementioned.

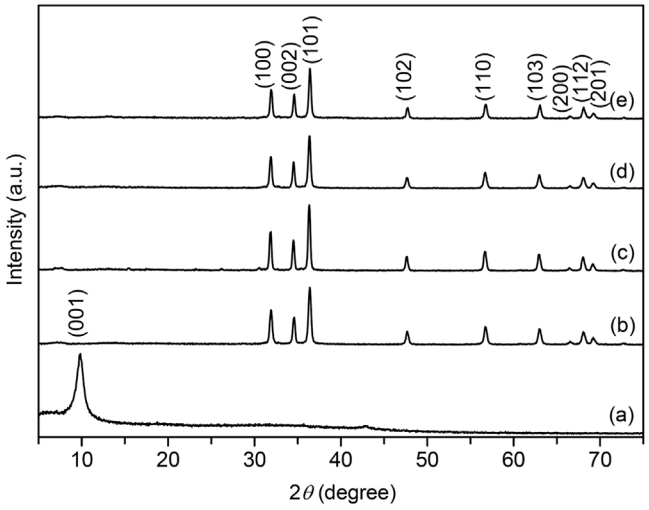

Fig. 2. XRD patterns of (a) GO, (b) ZnO, (c), rGO(0.4,24)-ZnO, (d) rGO(4,6)-ZnO, and (e) rGO(13,6)-ZnO samples.

Amount of added GO in the rGO-ZnO sample was clarified by TGA. As shown in Fig. S1, TGA curves represented GO, ZnO, and the rGO(0.4,24)-ZnO sample. GO showed several stages of decomposition. Upon heating below 100 °C, the weight loss was mainly associated to the adsorbed water. Two significant stage drops in weight were observed around 226 and 541 °C. The initial stage was belong to the decomposition of the labile oxygen-containing functional groups, while the final stage involved the breaking bond of C—C graphitic structure due to pyrolysis of the carbon skeleton of GO [36–38]. On the other hand, there was no significant drop of weight observed on ZnO sample even when the temperature reached 800 °C, indicating that the ZnO was thermally stable. As for the rGO(0.4,24)-ZnO sample, the total weight loss from 250 to 800 °C was determined to be around 3%. This value was pretty close to the real amount of GO added to the ZnO as depicted in the synthesis procedure.

Morphology of GO, ZnO and rGO(0.4,24)-ZnO composites was investigated by TEM. As shown in Fig. 4(a), few-layered sheets were observed on the GO, suggesting an exfoliation of oxygen functional groups such as epoxy and enriched phenolic compounds appeared on the basal plane [35]. ZnO showed rod-like shaped morphology (Fig. 4(b)), in good agreement with its preferred orientation suggested from its XRD pattern. Shown in Fig. 4(c) is the TEM image of the rGO(0.4,24)-ZnO sample. The presence of both rGO sheets and ZnO can be observed, where the rod shaped ZnO was mainly retained after the photocatalytic reduction process.

3.3. Optical properties

Optical properties of GO, ZnO and rGO(0.4,24)-ZnO composites were studied by DR UV–vis and fluorescence spectroscopies and shown in Fig. 5 and 6, respectively. As displayed in Fig. 5, GO

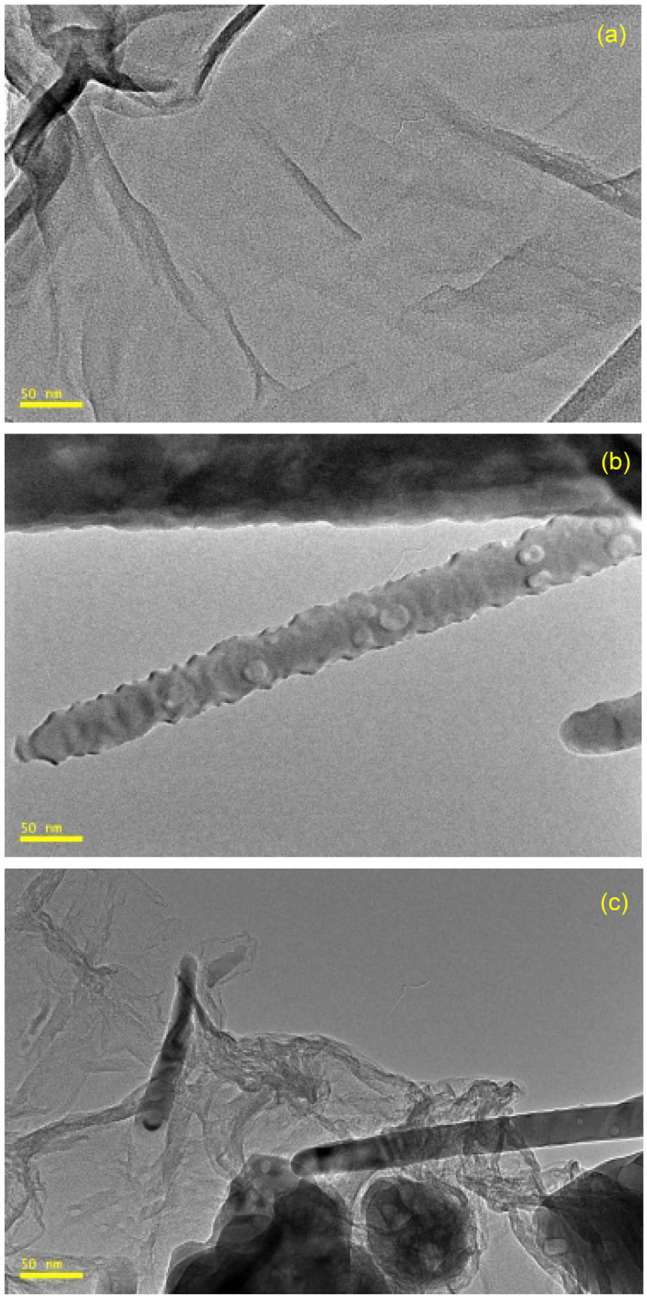

Fig. 4. TEM images of (a) GO, (b) ZnO, and (c) rGO(0.4,24)-ZnO samples. Scale bar shows 50 nm.

exhibited a broad peak up to visible region. The center of the peak can be observed at 345 nm that can be originated from the C=O groups. ZnO showed absorption up to 400 nm with the absorption peak was centered at 290 nm, whereas rGO(0.4,24)-ZnO sample gave similar absorption peak to that of the ZnO, but with additional absorption at the background level above 400 nm in a visible region as also reported elsewhere [26,29,34]. The increasing of background absorption in the visible region strongly suggested the existence of rGO. However, since the photocatalytic degradation of phenol in this study was conducted under UV light reaction only, such improvement of background absorption would not play a crucial role in enhancing the UV light activity. It was confirmed that the presence of small amount of rGO did not much alter the band structure of the ZnO.

Fig. 6 shows the emission spectra of ZnO and the rGO-ZnO samples which were monitored at excitation wavelength of 294 nm. As previously reported elsewhere [2–4,39], ZnO could give visible emission peaks. Two emission peaks were detected at 420 and 465 nm on the ZnO and all the rGO-ZnO samples, but the rGO-ZnO samples exhibited less emission intensity. Less emission intensity suggested the less electron-hole recombination on rGO-ZnO samples [28,34]. This result demonstrated that the rGO successfully suppressed the electron-hole recombination on the ZnO, which would be important for achieving high activity. Among the rGO-ZnO samples, the rGO-ZnO(0.4,24) sample exhibited significant lowest emission intensity, in good agreement with its highest photocatalytic activity.

3.4. Interfacial charge transfer and defect formation

As proposed above, good interaction between rGO and ZnO caused the less electron-hole recombination. Such interaction would not occur unless there are good interfacial charge transfers between them. The charge resistance of ZnO, rGO(0.4,24)-ZnO, rGO(4,6)-ZnO and rGO(13,6)-ZnO samples were studied by EIS. As displayed in Fig. 7, Nyquist plots gave a semicircle in the high frequency region that can be corresponded to the charge transfer resistance (R_{ct}). When the semicircle has a smaller arc radius, the R_{ct} value between the working electrode and electrolyte would be also smaller. This would indicate better electron conductivity and charge transfer capability [40,41]. It was clearly observed that all the rGO-ZnO samples exhibited a smaller semicircle than that of the ZnO, suggesting a smaller charge resistance appeared in the rGO-ZnO samples as compared to the ZnO alone. Employing a circuit model (constant phase element with diffusion model) and fitting by using a simplex model program (Fig. S2), R_{ct} values can be obtained. As shown in Table 2, ZnO, rGO(0.4,24)-ZnO, rGO(4,6)-ZnO and rGO(13,6)-ZnO gave R_{ct} values of 27.90, 19.95, 20.63, and 21.76 kΩ, respectively. These results demonstrated the significant role of rGO to decrease the charge resistance of ZnO. Again, the rGO(0.4,24)-ZnO showed superior property, *i.e.*, less charge resistance than other rGO-ZnO samples.

Less charge resistance suggested the better charge transfer rate and charge conductivity. Eq. (1) was employed to calculate the heterogeneous electron-transfer rate constant (k).

$$k = \frac{RT}{n^2F^2AR_{ct}C^0} \quad (1)$$

where R refers to the gas constant, T is temperature (K), n represents the number of transferred electrons per molecule of the redox probe, F shows the Faraday constant, A is the area of the electrode used (cm^2), R_{ct} is the charge transfer resistance, and C^0 is the concentration of redox couples in the bulk solution [40,42]. Table 2 also shows the k values of ZnO, rGO(0.4,24)-ZnO, rGO(4,6)-ZnO and rGO(13,6)-ZnO, which were determined to be 3.04×10^{-5}, 4.25×10^{-5}, 4.11×10^{-5} and 3.89×10^{-5} cm s^{-1}, respectively. It was obvious that the electron transfer on the rGO-ZnO samples occurred faster than the ZnO. Moreover, the rGO(0.4,24)-ZnO showed the fastest electron transfer among them.

In addition to the impedance data, Warburg impedance (W_d) can be obtained from the Nyquist plot in the low frequency region [40,41]. W_d value reflected the ion diffusion at the interface of electrode-electrolyte. The lower the W_d, the better the diffusion since there was less resistance on the ions flowing at the interface. The obtained W_d values for ZnO, rGO(0.4,24)-ZnO, rGO(4,6)-ZnO and rGO(13,6)-ZnO were 1.83×10^{-4}, 1.65×10^{-4}, 1.7×10^{-6} and 1.73×10^{-6} ($Ss^{1/2}$), respectively, as shown in Table 2. It was demonstrated that the rGO-ZnO samples have smaller W_d value than the bare ZnO. Meanwhile, the rGO(0.4,24)-ZnO showed

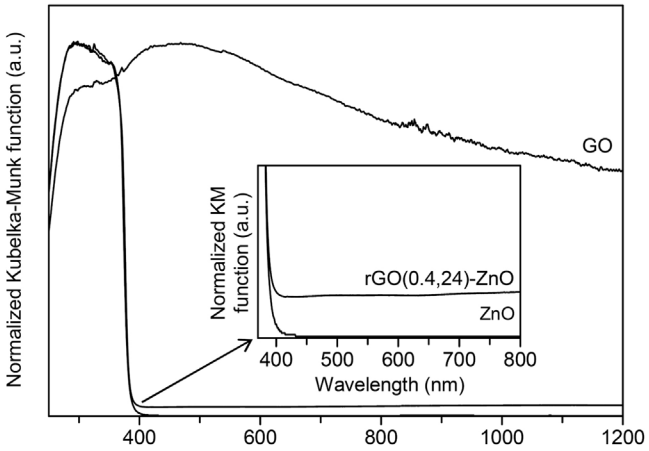

Fig. 5. DR UV–vis spectra of GO, ZnO, and rGO(0.4,24)-ZnO samples.

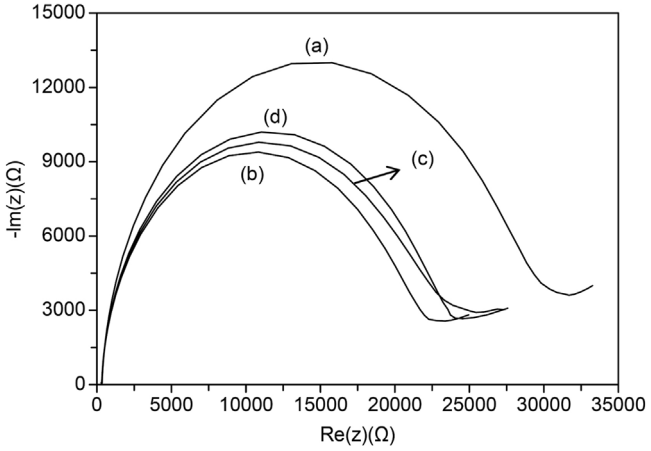

Fig. 7. EIS investigations on (a) ZnO, (b) rGO(0.4,24)-ZnO, (c) rGO(4,6)-ZnO, and (d) rGO(13,6)-ZnO samples.

smaller W_d value or better diffusion than the other rGO-ZnO samples. These results again supported that the rGO was able to facilitate the electron transfers.

It was clear that the rGO-ZnO(0.4,24) sample gave the highest photocatalytic activity owing to the lowest electron-hole recombination, less charge transfer resistance, fastest electron transfer rate, and fastest diffusion. Therefore, the importance of using optimized light intensity (0.4 mW cm^{-2}) and exposure time (24 h) in the synthesis part shall be further clarified. Since these synthesis parameters might affect the defect structures of the formed rGO basal plane, a Raman spectroscopy was used to investigate them. Displayed in Fig. 8 is the Raman spectra of graphite, GO and rGO-ZnO samples. Graphite showed two typical characteristics bands of graphite, which were the D and the G bands, as observed at around 1354 and 1575 cm^{-1}, respectively (Fig. 8(a)). It has been generally accepted that the D band is resulted from the break in the hexagonal graphitic lattice, whereas the G band is assigned to the in-plane stretching from symmetric sp^2 C—C network carbon [43]. GO and rGO-ZnO samples showed the D and the G peaks at around 1358 and 1583 cm^{-1}, respectively.

Defect ratio on the graphite basal plane can be determined by comparing the intensity of D to G peak (I_D/I_G) as listed in Table 2. As also shown in Fig. 8(a) and (b), graphite sample gave the I_D/I_G value of 0.82, while GO sample gave the I_D/I_G value of 0.96, indicating that GO was less crystalline with more defects than the graphite. This result was reasonable since the oxidation process led to the defect formation such as the introduction of oxygen functionalities. After UV-assisted photoreduction process using 0.4 mW cm^{-2} for 24 h, it was revealed that a certain restoration and self-healing process of sp^2 C—C bonds occurred since the I_D/I_G was slightly decreased to 0.94 (Fig. 8(c)). However, employing higher light intensities of 4 and 13 mW cm^{-2} for 6 h synthesis processes induced more defects as evidenced with the increase of the I_D/I_G values from 0.94 to 0.99 and 1.00, respectively. It was suggested that under exposure of high light intensity, the ZnO photocatalyst would also reduce some of oxygen functionalities, creating defects on the basal plane. From these results, it was obvious that the low light intensity was crucial to prevent further reduction process and enough exposure time (24 h) was required due to such low intensity. Since the formation of defects could impede the charge transfer between rGO and ZnO, the lower amount of defects would be one important factor that contributed to the higher photocatalytic activity.

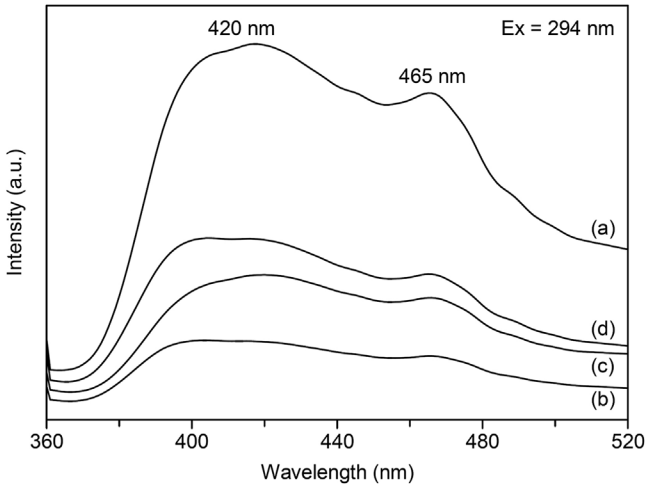

Fig. 6. Emission spectra of (a) ZnO, (b), rGO(0.4,24)-ZnO, (c) rGO(4,6)-ZnO, and (d) rGO(13,6)-ZnO samples.

3.5. Photocurrent study and photostability

To provide another evidence to confirm that the rGO-ZnO gave better interfacial charge transfer than the ZnO, transient photocurrent studies were conducted on the ZnO and the rGO(0.4,24)-ZnO for five cycles under exposure of UV light. The measurement was taken after 100 s for the stabilization of the electrode/electrolyte. As depicted in Fig. 9, it can be observed that both samples showed similar behaviour when the light was turned on and off. When the light was turned on, the photocurrent density increased rapidly, but it decreased fast to zero without the light. These phenomena clearly suggested that the ZnO and the rGO (0.4,24)-ZnO are both light-responsive materials. The higher photocurrent density was obtained on the rGO(0.4,24)-ZnO than the ZnO, suggesting that the rGO(0.4,24)-ZnO showed better electron conductivity than the ZnO. Furthermore, while the rGO (0.4,24)-ZnO showed more stable photocurrent, the ZnO gave decayed photocurrent density after a few on-off cycles.

The photostability of the ZnO and the rGO(0.4,24)-ZnO photocatalyst were further investigated under the similar reaction conditions in three consecutive reactions. The ZnO showed a significant loss on the photocatalytic activity, where the percentage degradation of phenol dropped from 9 to 5 and finally 2% after

Table 2
Comparisons of charge transfer resistance, heterogeneous electron transfer rate constant, Warburg impedance, and the intensity ratio of D to G peak.

Entry	Sample	R_{ct} (kΩ)	k (cm s^{-1})	W_d ($Ss^{1/2}$)	I_D/I_G
1	ZnO	27.90	3.04×10^{-5}	1.83×10^{-4}	–
2	rGO(0.4,24)-ZnO	19.95	4.25×10^{-5}	1.65×10^{-4}	0.94
3	rGO(4,6)-ZnO	20.63	4.11×10^{-5}	1.7×10^{-6}	0.99
4	rGO(13,6)-ZnO	21.76	3.89×10^{-5}	1.73×10^{-6}	1.00
5	Graphite	–	–	–	0.82
6	GO	–	–	–	0.96

the third cycle. On the other hand, the rGO(0.4,24)-ZnO photocatalyst showed more stable photocatalytic activity of 31, 28, and 27% after three cycle experiments. As shown in Fig. S3, after three successive cycles, ZnO showed less diffraction peak intensity, suggesting that ZnO suffered from photocorrosion under UV light exposure. In contrast, the rGO(0.4,24)-ZnO did not show much changes in the intensity. Since the structure of the rGO(0.4,24)-ZnO was remained stable after the reaction, it can be used as one potential photocatalyst for degradation of phenol. This study demonstrated that besides improving the photocatalytic performance of ZnO, the rGO was also found to increase the stability of the ZnO.

In order to evaluate the performance of rGO-ZnO in comparison with other reported photocatalysts, the comparisons shall be made to those carried out under similar photocatalytic reaction conditions, such as under low light intensity and similar initial concentration of phenol. When comparing ZnO with TiO_2, ZnO seems to give lower photocatalytic activity of 9% degradation after 6 h, while TiO_2 having the mixture of anatase-rutile gave 7% degradation in shorter reaction time of 3 h [44]. However, when comparing the enhancement after the bare photocatalyst was modified with rGO, the current rGO-ZnO gave larger improvement (3.4 times) than that of the reported rGO-TiO_2 (2.4 times). This result shows that the current approach to optimize both light intensity and exposure time is a good method to optimize the photocatalytic activity of rGO-ZnO. Only considering the activity improvement after addition of rGO, the current optimized rGO-ZnO also gave better improvement than the reported rGO-carbon nitride (2.8 times) [40]. Even though the activity of ZnO was increased with the presence of rGO, further activity enhancement

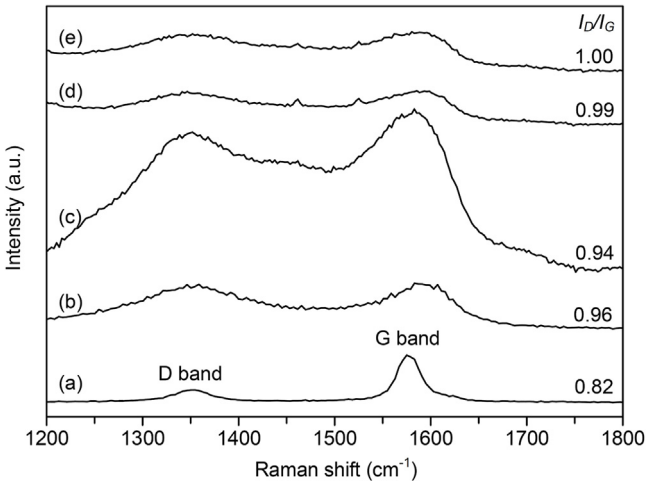

Fig. 8. Raman spectra of (a) graphite, (b) GO, (c) rGO(0.4,24)-ZnO, (d) rGO(4,6)-ZnO, and (e) rGO(13,6)-ZnO samples and their respective I_D/I_G values.

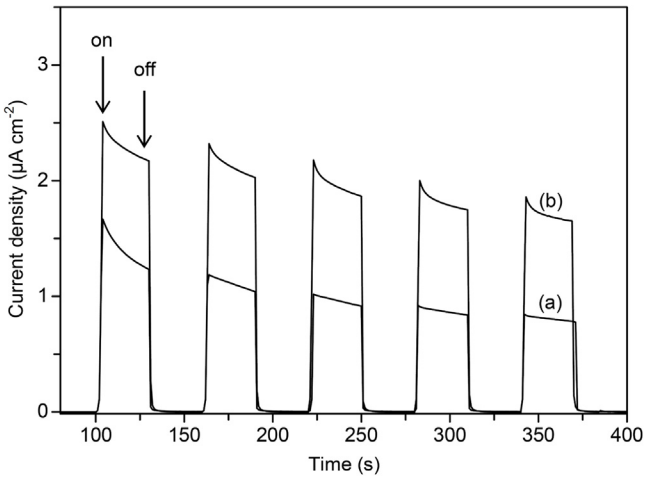

Fig. 9. Transient photocurrent responses of (a) ZnO and (b) rGO(0.4,24)-ZnO under UV light irradiation.

on the rGO-ZnO composite is still highly required. Since the efficient electron transfer rate greatly affected the activity, improving the system by using electron transfer and interfacial mediators would be one of the best approaches to prolong the lifetime of photogenerated charge carriers and promote the transfer efficiency of charge carriers across the interface between rGO and ZnO.

4. Conclusions

Contributions of light intensity and duration time in the photocatalytic reduction of GO over ZnO to produce rGO-ZnO composites were examined. Optimum performance of the rGO-ZnO was achieved when using low light intensity (0.4 mW cm^{-2}) and enough exposure time (24 h). These conditions were proposed to be crucial to form rGO with low amount of defects as proposed by the Raman spectroscopy. The formation of rGO with low amount of defect contributed in suppressing the electron-hole recombination, leading to low charge transfer resistance, fast diffusion and high electron transfer rate on the ZnO. As the result, the rGO (0.4,24)-ZnO sample not only gave around three times higher photocatalytic activity, but also better photocatalytic stability than the ZnO.

Acknowledgements

This work was financially supported by the Ministry of Higher Education (MOHE, Malaysia) and Universiti Teknologi Malaysia (UTM, Malaysia) through the Research University Grant (Tier 1, cost center code: Q.J130000.2509.06H66). F. H acknowledges the support of UTM through the Zamalah scholarship.

Appendix A. Supplementary data

Supplementary data associated with this article can be found, in the online version, at http://dx.doi.org/10.1016/j.jphotochem.2017.03.016.

References

[1] S.K. Pardeshi, A.B. Patil, A simple route for photocatalytic degradation of phenol in aqueous zinc oxide suspension using solar energy, Sol. Energy 8 (2008) 700–705.
[2] K.M. Lee, C.W. Lai, K.S. Ngai, J.C. Juan, Recent developments of zinc oxide based photocatalyst in water treatment technology: a review, Water Res. 88 (2016) 428–448.

[3] S. Suwanboon, P. Amornpitoksuk, N. Muensit, Dependence of photocatalytic activity on structural and optical properties of nanocrystalline ZnO powders, Ceram. Int. 37 (2011) 2247–2253.
[4] D. Liu, Y. Lv, M. Zhang, Y. Liu, Y. Zhu, R. Zong, Y. Zhu, Defect-related photoluminescence and photocatalytic properties of porous ZnO nanosheets, J. Mater. Chem. A 2 (2014) 15377–15388.
[5] J. Xie, H. Wang, M. Duan, L. Zhang, Synthesis and photocatalysis properties of ZnO structures with different morphologies via hydrothermal method, Appl. Surf. Sci. 257 (2011) 6358–6363.
[6] J.B. Zhong, J.Z. Li, Z.H. Xiao, W. Hu, X.B. Zhou, X.W. Zheng, Improved photocatalytic performance of ZnO prepared by sol-gel method with the assistance of CTAB, Mater. Lett. 91 (2013) 301–303.
[7] L.-Y. Yang, S.-Y. Dong, J.-H. Sun, J.-L. Feng, Q.-H. Wu, S.-P. Sun, Microwave-assisted preparation, characterization and photocatalytic properties of a dumbbell-shaped ZnO photocatalyst, J. Hazard. Mater. 179 (2010) 438–443.
[8] C.A.K. Gouvêa, F. Wypych, S.G. Moraes, N. Durán, N. Nagata, P. Peralta-Zamora, Semiconductor-assisted photocatalytic degradation of reactive dyes in aqueous solution, Chemosphere 40 (2000) 433–440.
[9] S. Sakthivel, B. Neppolian, M.V. Shankar, B. Arabindoo, M. Palanichamy, V. Murugesan, Solar photocatalytic degradation of azo dye: comparison of photocatalytic efficiency of ZnO and TiO_2, Sol. Energy Mater. Sol. Cells 73 (2003) 65–82.
[10] C. Tian, Q. Zhang, A. Wu, M. Jiang, Z. Liang, B. Jiang, H. Fu, Cost-effective large-scale synthesis of ZnO photocatalyst with excellent performance for dye photodegradation, Chem. Commun. 48 (2012) 2858–2860.
[11] C. Han, M.-Q. Yang, B. Weng, Y.-J. Xu, Improving the photocatalytic activity and anti-photocorrosion of semiconductor ZnO by coupling with versatile carbon, Phys. Chem. Chem. Phys. 16 (2014) 16891–16903.
[12] F. Hussin, H.O. Lintang, L. Yuliati, Enhanced activity of C_3N_4 with addition of ZnO for photocatalytic removal of phenol under visible light, Malaysian J. Anal. Sci. 20 (2016) 102–110.
[13] V. Etacheri, R. Roshan, V. Kumar, Mg-doped ZnO nanoparticles for efficient sunlight-driven photocatalysis, ACS Appl. Mater. Interfaces 4 (2012) 2717–2725.
[14] R. Mohan, K. Krishnamoorthy, S.-J. Kim, Enhanced photocatalytic activity of Cu-doped ZnO nanorods, Solid State Commun. 152 (2012) 375–380.
[15] R. Georgekutty, M.K. Seery, S.C. Pillai, A highly efficient Ag-ZnO photocatalyst: synthesis, properties, and mechanism, J. Phys. Chem. C 112 (2008) 13563–13570.
[16] M.T. Uddin, Y. Nicolas, C. Olivier, T. Toupance, L. Servant, M.M. Müller, H.-J. Kleebe, J. Ziegler, W. Jaegermann, Nanostructured SnO_2-ZnO heterojunction photocatalysts showing enhanced photocatalytic activity for the degradation of organic dyes, Inorg. Chem. 51 (2012) 7764–7773.
[17] G.C.C. Yang, S.-W. Chan, Photocatalytic reduction of chromium(VI) in aqueous solution using dye-sensitized nanoscale ZnO under visible light irradiation, J. Nanopart. Res. 11 (2009) 221–230.
[18] A.K. Geim, K.S. Novoselov, The rise of graphene, Nat. Mater. 6 (2007) 183–191.
[19] M.A. Rafiee, J. Rafiee, Z. Wang, H. Song, Z.-Z. Yu, N. Koratkar, Enhanced mechanical properties of nanocomposites at low graphene content, ACS Nano 3 (2009) 3884–3890.
[20] A.A. Balandin, S. Ghosh, W. Bao, I. Calizo, D. Teweldebrhan, F. Miao, C.N. Lau, Superior thermal conductivity of single-layer graphene, Nano Lett. 8 (2008) 902–907.
[21] Z.-S. Wu, W. Ren, L. Gao, J. Zhao, Z. Chen, B. Liu, D. Tang, B. Yu, C. Jiang, H.-M. Cheng, Synthesis of graphics sheets with high electrical conductivity and good thermal stability by hydrogen arc discharge exfoliation, ACS Nano 3 (2009) 411–417.
[22] M.A. Worsley, S.O. Kucheyev, H.E. Mason, M.D. Merrill, B.P. Mayer, J. Lewicki, C. A. Valdez, M.E. Suss, M. Stadermann, P.J. Pauzauskie, J.H. Satcher, J. Biener, T.F. Baumann, Mechanically robust 3D graphene macroassembly with high surface area, Chem. Commun. 48 (2012) 8428–8430.
[23] K.I. Bolotin, K.J. Sikes, Z. Jiang, M. Klima, G. Fudenberg, J. Hone, P. Kim, H.L. Stormer, Ultrahigh electron mobility in suspended graphene, Solid State Commun. 146 (2008) 351–355.
[24] Y. Min, K. Zhang, W. Zhao, F. Zheng, Y. Chen, Y. Zhang, Enhanced chemical interaction between TiO_2 and graphene oxide for photocatalytic decolorization of methylene blue, Chem. Eng. J. 193–194 (193) (2012) 203–210.
[25] B. Li, T. Liu, Y. Wang, Z. Wang, ZnO/graphene-oxide nanocomposite with remarkably enhanced visible-light-driven photocatalytic performance, J. Colloid Interface Sci. 377 (2012) 114–121.
[26] T. Lv, L. Pan, X. Liu, T. Lu, G. Zhu, Z. Sun, Enhanced photocatalytic degradation of methylene blue by ZnO-reduced graphene oxide composite synthesized via microwave-assisted reaction, J. Alloys Compd. 509 (2011) 10086–10091.
[27] N. Kumar, A.K. Srivastava, H.S. Patel, B.K. Gupta, G.D. Varma, Facile synthesis of ZnO–reduced graphene oxide nanocomposites for NO_2 gas sensing applications, Eur. J. Inorg. Chem. (2015) 1912–1923.
[28] X. Zhou, T. Shi, H. Zhou, Hydrothermal preparation of ZnO-reduced graphene oxide hybrid with high performance in photocatalytic degradation, Appl. Surf. Sci. 258 (2012) 6204–6211.
[29] Z. Zhan, L. Zheng, Y. Pan, G. Sun, L. Li, Self-powered, visible-light photodetector based on thermally reduced graphene oxide-ZnO (rGO-ZnO) hybrid nanostructure, J. Mater. Chem. 22 (2012) 2589–2595.
[30] W. Feng, Y. Wang, J. Chen, L. Wang, L. Guo, J. Ouyang, D. Jia, Y. Zhou, Reduced graphene oxide decorated with in-situ growing ZnO nanocrystals: facile synthesis and enhanced microwave absorption properties, Carbon 108 (2016) 52–60.
[31] B. Weng, M.-Q. Yang, N. Zhang, Y.-J. Xu, Toward the enhanced photoactivity and photostability of ZnO nanospheres *via* intimate surface coating with reduced graphene oxide, J. Mater. Chem. A 2 (2014) 9380–9389.
[32] A.A. Ashkarran Williams, B. Mohammadi, ZnO nanoparticles decorated on graphene sheets through liquid arc discharge approach with enhanced photocatalytic performance under visible-light, Appl. Surf. Sci. 342 (2015) 112–119.
[33] G. Williams, P.V. Kamat, Graphene-semiconductor nanocomposites: excited-state interactions between ZnO nanoparticles and graphene oxide, Langmuir 25 (2009) 13869–13873.
[34] X. Liu, L. Pan, Q. Zhao, T. Lv, G. Zhu, T. Chen, T. Lu, Z. Sun, C. Sun, UV-assisted photocatalytic synthesis of ZnO–reduced graphene oxide composites with enhanced photocatalytic activity in reduction of Cr(VI), Chem. Eng. J. 183 (2012) 238–243.
[35] D.C. Marcano, D.V. Kosynkin, J.M. Berlin, A. Sinitskii, Z. Sun, A. Slesarev, L.B. Alemany, W. Lu, J.M. Tour, Improved synthesis of graphene oxide, ACS Nano 4 (2010) 4806–4814.
[36] P. Song, X. Zhang, M. Sun, X. Cui, Y. Lin, Synthesis of graphene nanosheets via oxalic acid-induced chemical reduction of exfoliated graphite oxide, RSC Adv. 2 (2012) 1168–1173.
[37] S. Stankovich, D.A. Dikin, R.D. Piner, K.A. Kohlhaas, A. Kleinhammes, Y. Jia, Y. Wu, S.T. Nguyen, R.S. Ruoff, Synthesis of graphene-based nanosheets via chemical reduction of exfoliated graphite oxide, Carbon 45 (2007) 1558–1565.
[38] C. Tao, X. Zou, Z. Hu, H. Liu, J. Wang, Chemically functionalized graphene/polymer nanocomposites as light heating platform, Polym. Composite 37 (2016) 1350–1358.
[39] D. Das, P. Mondal, Photoluminescence phenomena prevailing in c-axis oriented intrinsic ZnO thin films prepared by RF magnetron sputtering, RSC Adv. 4 (2014) 35735–35743.
[40] P. Tiong, H.O. Lintang, S. Endud, L. Yuliati, Improved interfacial charge transfer and visible light activity of reduced graphene oxide–graphitic carbon nitride photocatalysts, RSC Adv. 5 (2015) 94029–94039.
[41] J. Li, X. Liu, L. Pan, W. Qin, T. Chen, Z. Sun, MoS_2–reduced graphene oxide composites synthesized via a microwave-assisted method for visible-light photocatalytic degradation of methylene blue, RSC Adv. 4 (2014) 9647–9651.
[42] M. Chirea, J. Borges, C.M. Pereira, A.F. Silva, Density-dependent electrochemical properties of vertically aligned gold nanorods, J. Phys. Chem. C 114 (2010) 9478–9488.
[43] K.N. Kudin, B. Ozbas, H.C. Schniepp, R.K. Prud'homme, I.A. Aksay, R. Car, Raman spectra of graphite oxide and functionalized graphene sheets, Nano Lett. 8 (2008) 36–41.
[44] N.S. Alim, H.O. Lintang, L. Yuliati, Photocatalytic removal of phenol over titanium dioxide-reduced graphene oxide photocatalyst, IOP Conf. Ser.: Mater. Sci. Eng. 107 (2016) 7 012001.